JP2.4 SENSITIVITY STUDY OF THE GLOBAL CONTRAILS RADIATIVE FORCING AND CRYSTALS OPTICAL PROPERTIES DUE TO PARTICLE SHAPE.

Krzysztof M. Markowicz[*1], Marcin Witek[2]
[1]Institute of Geophysics, University of Warsaw, Warszawa, Poland
[2]California Institute of Technology, Pasadena, USA

1. INTRODUCTION

Aviation influences the Earth's atmosphere trough the emission of gases and particles which in turn affect climate both directly and indirectly. Water vapor and aerosol particles acting as cloud condensation nuclei are of special interest because they support cloud formation and modify cloud properties. Water vapour emitted by aircrafts perturbs the background humidity in the atmosphere and can lead to the formation of contrails (line-shaped contrails) or the "air-traffic-induced cirrus cloud" (Sausen et al., 2005). A climate effect measured by the radiative forcing (RF) of contrail clouds is highly uncertain due to a limited number of observations and difficulties with parameterization of contrails in global climate models (Dietmüller et al., 2008; Ponater et al., 2002). The Intergovernmental Panel on Climate Change (IPCC) special report "Aviation and Global Atmosphere" (Penner et al. 1999) provided an estimate for the RF of linear contrails in the range of 0.02 W/m^2 for 1992, amounting 40% of the total RF from aviation impact. The IPCC emphasises that the RF due to line-shaped contrails is sufficiently known to be attribute at least a "fair" level of scientific understanding. The TREDEOFF project in 2005 led to updates in the IPCC's value. The new studies gave 0.01 W/m^2 as the best estimate of mean global contrail RF in 2000 (Sausen et al., 2005). The last IPCC report (2007) maintained 0.01 W/m^2 for the global mean forcing but attributed to it a "low" level of scientific understanding. However, one may expect contrails to have stronger impact on a regional scale than on a global scale. Minnis et al. (1999), by studying the RF changes for aircraft fuel consumption scenarios for the years 1992 and 2050, show that the zonal mean forcing at northern mid-latitudes is five times larger than the global mean. The computed global mean RF by line-shaped contrails is ~0.02 Wm^{-2} in 1992 and ~0.1 Wm^{-2} in 2050 (Minnis et al., 1999).

A major problem in the modelling of optical properties of contrails is the nonspericity of ice crystals forming these clouds. That prevents efficient analytical treatment of their single scattering properties. However, for the shortwave (SW) radiation range most ice particles are considerably larger than the wavelengths of the incoming solar radiation. Therefore, the geometric optics approximation offers a conceptually simple way to simulate scattering by almost arbitrarily shaped objects. Unfortunately, ice particles are too small to apply geometric methods in the longwave (LW) range. The LW single-scattering parameters are computed from composite methods based on the finite-difference time-domain (FTTD) technique (Sun et al., 1999; Yang and Liou, 1996), geometric-optics method and the Lorentz-Mie solution (Bohren, and Huffmann, 1983) for equivalent spheres (Yang et al., 2005); the T-matrix method (Mishchenko et al., 1994), and the discrete dipole approximation (DDA) method (Drain and Flatau 1994) for arbitrary particle shape. Among these methods, the T-matrix delivers an exact solution and is computationally efficient but is also restricted to rotationally symmetrical particles. In general, computations of ice optical properties for more complicated particle habits are very difficult and computationally inefficient. It is because scattering properties, such as the scattering and absorption cross-section, phase function, asymmetry parameter, and backscattering cross-section need to be evaluated

[*] *Corresponding author address*: Krzysztof M. Markowicz, Institute of Geophysics, University of Warsaw, Pasteura 7, 02093 Warsaw, Poland, e-mail: kmark@igf.fuw.edu.pl

many times for particles with various sizes, shapes and in random orientations against incoming radiation. The DDA technique has been successfully used by Liu (2008) in the microwave range for 11 particle shapes. Another studies and databases on ice and snow scattering properties in the microwave range using alternative computational methods can be found in Evan and Stephens (1995), Kim (2006), and Hong (2007). A similar database that covers near- to far-infrared spectrum regions has been reported by Yang et al. (2005), and visible- to near-infrared spectrum by Yang et al. (2000).

2. METHODOLOGY

2.1 *Radiative transfer model*

All calculations of RF were performed using a model which includes interface between the state-of-the-art radiative transfer model (RTM) Fu-Liou (Fu and Liou, 1992; Fu and Liou 1993) and databases containing optical properties of the atmosphere and surface reflectance and emissivity. This interface allows to determine radiative fluxes in the atmosphere and to estimate the contrails RF for clear and all sky (real clouds) conditions for various crystal shapes. We use the 200503 version of the Fu-Liou code which includes delta 2/4 stream solver (for SW and LW range) described by Fu and Liou (1992; 1993). This code is used to calculate radiative fluxes for following cases: clear sky, contrails, background clouds with and without contrails.

The Fu-Liou code includes 6 shortwave and 12 longwave spectral bands. For each band the correlated-k CKD_2.4 method (Fu and Liou, 1992) is used to calculate optical properties such as transmission and reflectance. The Fu-Liou code is fast therefore enables computation of radiative fluxes in 3D (global scale) domain. The comparison of the results accuracy of the FU-Liou code mentioned here with other more precise RTM techniques shows good agreement Myhre et al. (2009). However, it does not take into account 3D effect, e.g. cloud shading and horizontal inhomogeneity.

2.2 *Contrail cloud models*

Contrail clouds consist of ice crystals having a variety of shapes, sizes and volumes. Moreover, contrail clouds evolve in time undergoing changes in their crystal geometries and concentrations. In order to effectively assess their radiative effects, certain

	optical model	shape	model description
1	Flat optics	not defined	single scattering albedo 1 for SW and 0.6 for LW, asymmetry parameter 0.8.
2	Strauss contrails	Mixture	based on geometric optics in LW (hexagonal shapes) and Mie-calculations in SW (spheres).
3	Droxtal	droxtal	optical particles based on improved geometrical-optics method (Yang at al., 2005) in SW and finite-difference time-domain (Yang, et al., 2000), the T-matrix (Mishchenko and Travis, 1994) in LW. The particle's aspect ratio depends on the particle size
4	Plate	hexagonal plates	
5	Hex column	hexagonal columns	
6	DDA plates 0.2	hexagonal plates with aspect ratio 0.2	optical properties based on DDA (Drain and Flatau, 1994) in LW and geometric method (Macke and Mishchenko, 1996) in SW.
7	DDA plates 0.5	hexagonal plates with aspect ratio 0.5	
8	DDA hex 3	hexagonal columns with aspect ratio 3	
9	DDA hex 5	hexagonal columns with aspect ratio 5	
10	Mie spherical	homogenous spherical particles.	Lorenz-Mie theory

Table 1. Description of contrail cloud optical models used in this study.

simplifications regarding the shape and size distribution of particles forming these clouds have to be made. For such simplified contrail cloud models optical databases have to be established prior to RF calculations. We use 10 various contrail cloud models, listed in Table 1. Four of these models (6,7,8, and 9) required numerically expensive single-scattering derivations for individual ice crystals. Another four models (2,3,4,and 5) are based on optical databases found in the literature, and the remaining two (1,10) include highly simplified models, used here for reference.

2.3 *Model resolution*

Described in this section interface between the RTM and various databases of the optical properties and the meteorological data are used to compute the radiation fluxes at a regular grid with the horizontal resolution of 5x5 degree at 30 vertical lavels. The background fields such as the thermodynamic profiles, the surface albedo/emissivity and the cloud properties are averaged over 25-40 years to define climatology. Therefore all simulations presented in this paper are related to the mean condition. To reduced a large number of the RTM computations (365 diurnal cycles per year) we defined for each month so called „mean solar day". Afterwards 12 diurnal cycles at each horizontal grid point are computed. The time resolution is 20 min for the cases when the sun is above horizon and 3 h during the night. Such a time resolutions during the day are required to reach enough accuracy for the estimation of the mean diurnal solar flux (24 h).

3. SINGLE-SCATTERING PROPERTIES OF THE ICE CRYSTAL MODELS

In this section optical properties of some of the contrail cloud models listed in Table 1 are shortly analyzed. Fig. 1 shows the wavelength dependent and averaged over the size distribution single scattering albedo for 7 ice crystal models. We omitted some of the models (flat optics, DDA plates 0.5, and DDA hex 3) for a better clarity of the figures. An equivalent comparison but for the asymmetry parameter is presented in Fig. 2. Figs. 1-2 show that there are substantial differences in optical properties between the models. These differences result mostly from distinct ice habits and various aspect ratios among the contrail models. Various methods used to derive optical properties and related computational errors could also contribute to the observed spread, but these effects are difficult to determine. Differences in SSA reach up to 0.1 in the infrared range (Fig. 1), whereas the SW values are very similar between models due to small absorption in this range. The asymmetry parameter has larger variability, especially in the SW radiation regime (Fig. 2). The new models (denoted DDA Hex Col and DDA Hex Pla) with the fixed aspect ratios diverge from the previous estimates by Yang et al. (2000; 2004) and Strauss et al. (1997). The present simulations give the values of asymmetry parameter more similar to the ones obtained for spherical particles and higher by around 0.1 comparing to the other models. Due to the high energy density in the SW range we expect the simulated differences to have substantial impact on RF calculations.

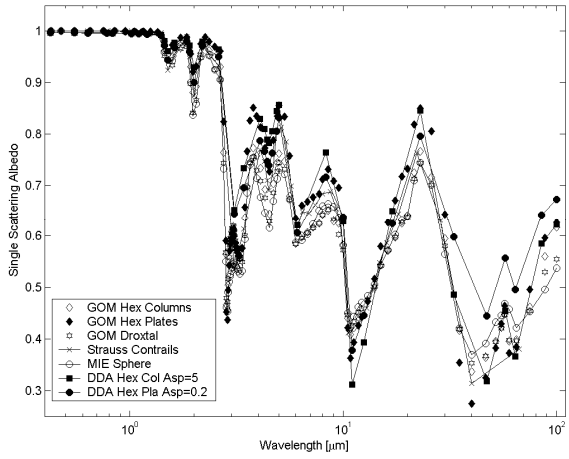

Fig. 1 Single scattering albedo as a function of wavelength for several contrail cloud models. The first three crystal types (open diamonds, solid diamonds and hexagrams) are based on Yang et al. (2000;2005) databases, the line with crosses shows contrails

properties taken from Strauss et al., (1997), the line with open circles marks optical properties for spherical particle computed from the Lohrenz-Mie theory, and the last two lines (with solid squares and solid circles) correspond to hexagonal column with aspect ratio 5 and hexagonal plate with aspect ratio 0.2 (models 9 and 6 in Table 1). Optical properties were averaged over ice crystal size distribution given by Strauss, et al. (1997).

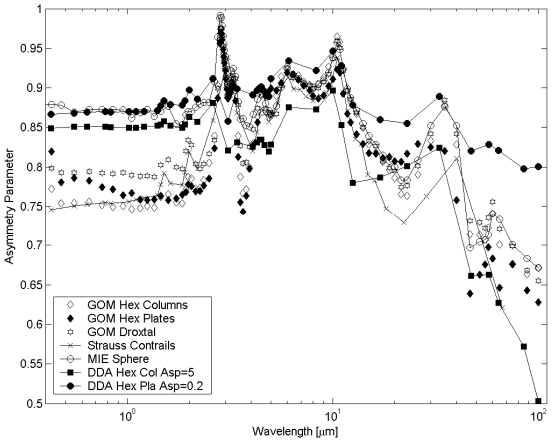

Fig. 2 The same as the Fig. 1 but for the asymmetry parameter.

4. SENSITIVITY OF THE RADIATIVE FORCING DUE TO THE CRYSTAL SHAPES

In order to calculate a geographic distribution of the global and the annual mean contrails RF the contrails cover must be determined. The two cases are discussed here: a 1% homogeneous contrail cover and the contrail cover provided by the AERO2K model (Rädel and Shine, 2008). The propose of the first case is the sensitivity study of the contrails RF due to the background conditions (clouds, temperature, humidity, surface albedo/emissivity). In case of the AERO2K model a more realistic contrails cover is taken into account. This model merging the AERO2K flight inventory (Eyers et al., 2004) and meteorological data and normalizing it to satellite observations. The contrails are fixed for the RTM computation at an altitude between 10 and 11 km about ground. For the 550 nm an optical depth of the contrail of 0.3 was chosen. This allowed to scale the particle extinction coefficient (defined for SW and LW spectrum range) from the crystal optical models discussed in section 2.

The contrails SW RF is determined mainly by the solar zenith angle, surface albedo, and their optical depth (Ebert and Curry, 1992). The aspherical particles cause a larger albedo than spherical ones (Kinne and Liou, 1989; Gayet et al., 1998). In general, the SW RF is negative and has a greater magnitude over dark surfaces than over bright surfaces. The contrails LW RF is highest when the clear-sky radiative flux in to space is large (i.e. larger over warm than over cool surfaces, larger in a dry than in a humid atmosphere) and the cloud emissivity is large (Ebert and Curry, 1992; Fu and Liou, 1993). However, the NET RF of contrails may be positive or negative; e.g. thin cirrus clouds cause a small but positive RF at the TOA and thick cirrus clouds may cause cooling (Stephens and Webster, 1981; Fu and Liou, 1993).

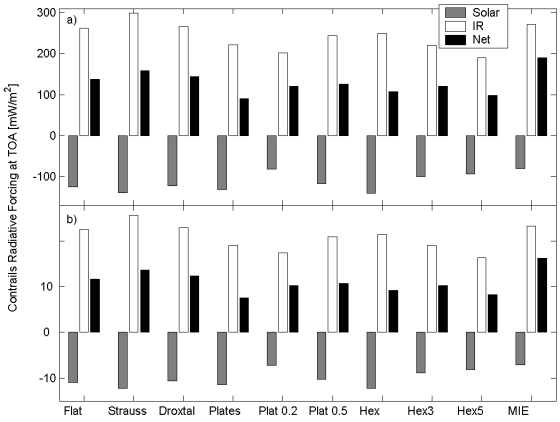

Fig. 3 Global and annual mean clear sky contrails RF at the top of the atmosphere for various ice crystal optical models listed in Table 1. Panel (a) corresponds to the homogenous 1% contrails cover. Panel (b) corresponds to contrails cover based on the AERO2K database.

Fig. 3 shows variability of the SW (grey bars), the LW (white bars), and the NET (black bars) contrails TOA RF depending on the particles shape. Panel (a) corresponds to the uniform 1% contrails cover and panel (b) to the contrails fraction provided by the AERO2K model. These simulations were performed for

the clear sky condition without any background cloud. The global annual mean of the contrails RF show large variability with crystal shape. The ratio of the standard deviation to the mean value is about 0.2 for SW, 0.14 for LW and 0.23 for NET. In both cases the largest NET RF is obtained for the spherical particles and for the Strauss's contrails. In contrary, the smallest value is found for the Yang's hexagonal plates and for the hexagonal columns with aspect ratio of 5 (model 9). The smallest (negative) SW RF is found for the spherical particles and the hexagonal plates with aspect ratio of 0.2. These results are consistent with the large asymmetry parameter for these type of crystal shape, which leads to a reduction of the negative forcing. The largest SW RF is found for the Strauss's contrails and the Yang's hexagonal particles. The variability of the contrails LW RF with particle shape is smaller and less pronounced. In this case the Strauss's contrails have the largest radiative effect and the Yang's hexagonal columns with aspect ratio of 5 the smallest one.

The global annual mean of contrails RF for 1% homogenous contrails cover and averaged over ten crystal model is -0.11 ± 0.02 W/m^2 for SW, 0.24 ± 0.03 W/m^2 for LW, and 0.13 ± 0.03 W/m^2 for NET under clear sky conditions and -0.07 ± 0.02 W/m^2 for SW, 0.20 ± 0.03 W/m^2 for LW, and 0.13 ± 0.02 for NET under all sky conditions. The uncertainties corresponds to the standard deviation due to the different optical model only. These simulations results are in agreement with previous studies, e.g. Myhre and Stordal (2001) report the clear sky RF of contrails, described according to Strauss et al., (1997) model, of -0.15, 0.27, and 0.12 W/m^2 for SW, LW, and NET, respectively. In case of the AERO2K contrails fraction are -9.9 ±1.9 mW/m^2 for SW, 20.9 ± 2.9 mW/m^2 for LW and 11.0 ± 2.6 mW/m^2 for NET under clear sky conditions and -5.7 ± 1.2 mW/m^2 for SW, 16.8± 2.4 mW/m^2 for LW, and 11.1±2.1 mW/m^2 for NET under all sky conditions (Table 2). The comparison of the average contrails radiation effect with other studies shows also good agreement, e.g. Myhre and Stordal (2001) report 11.0 mW/m^2; Sauses et al. (2005) reports 10 mW/m^2. However, our results are significant larger if compared to Rädel and Shine (2008) who estimated the contrails RF at the level of 6.4 mW/m^{2}for 2002.

crystal model	Clear sky			All sky		
	SW	LW	NET	SW	LW	NET
1	-10.9	22.5	11.7	-6.6	18.3	11.7
2	-12.2	25.6	13.6	-7.1	20.7	13.6
3	-10.6	22.9	12.3	-6.1	18.6	12.5
4	-11.4	19.0	7.6	-6.8	15.4	8.6
5	-7.2	17.4	10.2	-4.0	13.9	9.9
6	-10.2	20.9	10.7	-5.8	16.9	11.1
7	-12.2	21.4	9.2	-7.1	17.3	10.2
8	-8.8	19.0	10.2	-5.0	15.3	10.3
9	-8.1	16.4	8.3	-4.7	13.2	8.5
10	-7.1	23.3	16.2	-4.0	18.9	14.9
mean	**-9.9**	**20.9**	**11.0**	**-5.7**	**16.8**	**11.1**
std	**1.9**	**2.9**	**2.6**	**1.2**	**2.4**	**2.1**

Table 2. Global and annual mean clear sky and all sky the contrails SW, LW and NET RF [mW/m^2] at the top of the atmosphere in the case of the contrails cover obtained from the AERO2K database and the contrails optical depth of 0.3 at 500 nm.

5. ROLE OF BACKGROUND CLOUD FIELD IN THE CONTRAILS RADIATIVE FORCING

The results show significant sensitivity to the background clouds in the SW RF and the LW RF, while the effect of clouds for NET RF is almost balanced. Fig. 4 shows relative difference between all sky and clear sky NET RF in percentage as a function of the contrails optical depth. The calculation were performed for the Strauss's contrails optical model and the homogenous 1% contrails cover. For the contrails optical depth of less than 0.3 the clear sky forcing is slightly larger than the all sky one. For thicker contrails, cloudy conditions

lead to increase the NET RF. However, the effect of cloud is very small and for typical contrails optical depths do not exceed a few percent.

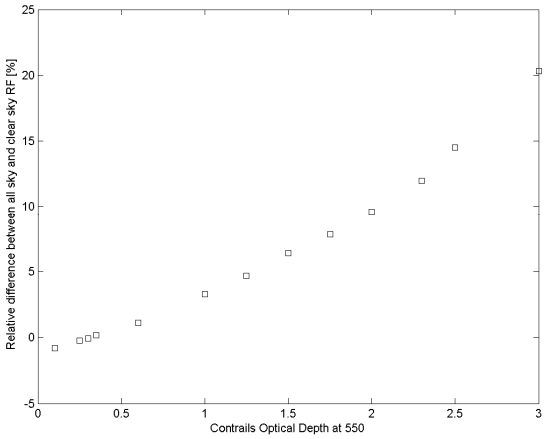

Fig.4 Relative difference between global and annual mean all sky and clear sky contrails NET RF in percentage as a function of optical depth for the Strauss's contrails optical model and the homogenous 1% contrails cover.

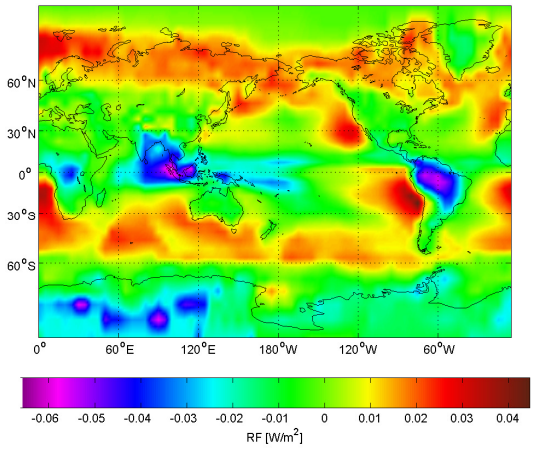

Fig. 5 All sky minus clear sky annual mean contrails NET RF for the Strauss's contrails and the optical depth 0.3 at 550 nm obtained for the homogenous 1% contrails cover.

Fig. 5 shows spatial distribution of the difference between all sky and clear sky annual mean NET RF. The simulations were performed for the Strauss's contrails with an optical depth of 0.3 at 550 nm and for the homogenous 1% contrails cover. Negative differences evident mainly in tropics (in the Inter-tropical Convergence Zone) as the cirrus clouds reduce the LW RF stronger than the SW RF. In the region of low level clouds the NET RF under the all sky conditions is larger in comparing with clear sky one. It can be explained by the fact that the low level clouds do not have a strong impact on the LW RF but significantly reduce negative SW RF due to the large albedo.

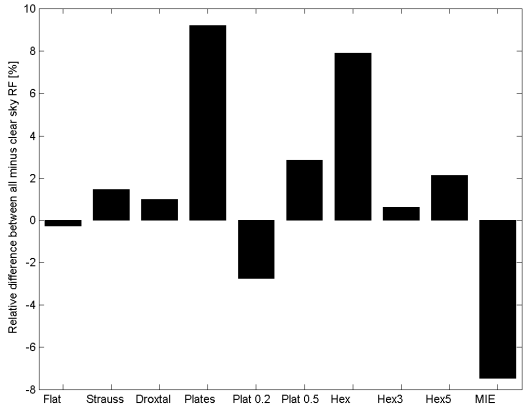

Fig. 6 Relative difference between the global and annual mean of the all sky minus the clear sky contrails NET RF efficiency at the top of the atmosphere for various ice crystal optical models and the homogenous 1% contrails cover.

To compare cloudiness effect on the contrails RF for various crystal shapes we computed a relative difference of the contrails RF between the all sky and the clear sky conditions and for contrails optical depth of 0.3 at 550 nm. The obtained RF differences vary from -7.5 to 9.2 % (Fig.6). For three models (flat optics, hexagonal pates with aspect ratio of 0.2, and spherical particles) this parameter is negative, which means that background clouds reduce the NET RF of contrails. This negative difference corresponds to the larger variation of the LW than the SW RF due to background cloud. Only for three models (hexagonal plates and columns and for spherical particles) difference of all and clear sky forcing significantly exceeds 2-3%. For remaining models the effect of background clouds seem negligible.

6. CONCLUSION

We found a large variation of the contrails RF with the particles shape as a result of significant differences in the particle single scattering properties. The results of global simulation show that the variability of the contrails RF with varying different crystal shape is about 20% for SW, 14% for LW, and 23% for NET under the clear sky condition and 22% for SW, 14% for LW, and 19% for NET under the all sky condition. Because contrails form under various surrounding thermodynamic and dynamic conditions their shapes are not uniform, what leads to the large uncertainties in the RF estimations.

We estimated the mean global contrails RF obtained for the realistic contrails cover taken from the AERO2K. The global annual mean contrails RF database (averaged over 10 crystal models applied here) are -5.7, 16.8, and 11.1 mW/m^2 for, SW, LW, and for NET, respectively. The simulations performed for the clear sky condition depict similar the NET RF (11.0 mW/m^2) but significantly stronger SW (-9.9 mW/m^2) and LW, (20.9 mW/m^2) RF if compared to the all sky case. Although the global contrails forcing is relatively small in any region of the high air traffic density can be 30-40 times larger, e.g. a maximum of RF over USA is about 0.44 W/m^2 and over Europe 0.32 W/m^2.

The cloudiness has only a small effect on the contrails RF, mostly due to an opposite effect in the SW and the LW spectral range. Magnitude of the reduction of the SW and the LW RF by cloud fields is similar. However, this effect is observed only for small optical depth, e.g. for contrails optical depth larger than 1 the all sky RF becomes significantly larger than clear sky one. In addition, a difference between the of all and clear sky RF depends strongly on the particle shapes.

7. ACKNOWLEDGMENTS

This work was partially funded by the EU within the QUANTIFY Integrated Project under the contract no. 003893 (GOCE) and by the Polish Ministry of Higher Education and Science Grant nr 31/6.PR UE/2006/7.

8. BIBLIOGRAPHY

Bohren, C. F. and D. R. Huffmann, 1983: Absorption and scattering of light by small particles. *Wiley-Interscience,* New York, 541 pp.

Dietmüller, S., M. Ponater, R. Sausen, K. P. Hoinka, and S. Pechtl, 2008: Contrails, Natural Clouds, and Diurnal Temperature Range. *J. Climate*, **21**, 5061–5075.

Drain, B. T., and P. J. Flatau, 1994: Discrete-dipole approximation for scattering calculations. *J. Opt. Soc. Am. A*, **11**, 1491–1499.

Ebert, E. E. and J. A. Curry, 1992: A parameterization of ice cloud optical properties for climate models. *J. Geophys. Res.*, **97**, 3831-3836.

Evans K., and G. L. Stephens, 1995: Microwave Radiative Transfer trough Clouds Composed of Realistically Shaped Ice Crystals. Part I: Single Scattering Properties, *J. Atmos. Sci.*, **52**, 2041-2057 .

Eyers, C. J., P. Norman, J. Middel, M. Plohr, S. Michot, K. Atkinson, and R. A. Christou, 2004: AERO2K Global aviation emissions inventories for 2002 and 2025, *Tech. Rep. QINETIQ/04/01113*, QinetiQ Ltd., Farnborough, UK.

Fu, Q. and K.-N. Liou, 1992: On the correlated k-distribution method for radiative transfer in nonhomogenous atmospheres, *J. Atmos. Sci.,* **49**, 2139-2156.

Fu, Q. and K. Liou 1993: Parameterization of the radiative properties of cirrus clouds. *J. Atmos. Sci.*, *50*, 2008–2025.

Gayet, J.-F., F. Auriol, S. Oshchepkov, F. Schröder, C. Duroure, G. Febvre, J.-F. Fournol, O. Crépel, P. Personne, and D. Daugereon, 1998: In situ measurements of the scattering phase function

of stratocumulus, contrails and cirrus, *Geophys. Res. Lett.,* **25**, 971-974.

Hong, G., 2007: Parameterization of scattering and absorption properties of nonspherical ice crystals at microwave frequencies. *J. Geophys. Res.*, **112**, D11208.

IPCC, 2007: Climate Change 2007: The scientific basis-contribution of Working Group I to the fourth assessment report of the Intergovernmental Panel on Climate Change, *Cambridge Univ. Press*, New York, 996 pp.

Kim, M.-J., 2006: Single scattering parameters of randomly oriented snow particles at microwave frequencies. *J. Geophys. Res.,* **111***,* D14201, doi:10.1029/2005JD006892.

Kinne, S. and K. N. Liou, 1989: The effects of the nonsphericity and size distribution of ice crystals on the radiative properties of cirrus clouds, . *Atmos. Res.,* **24,** 273–284.

Liu, G., 2008: A Database of Microwave Single-Scattering Properties for Nonspherical Ice Particles. *Bull. Amer. Meteor. Soc.*, **89**, 1563–1570.

Macke, A., and M. I. Mishchenko, 1996: *Applicability of regular particle shapes in light scattering calculations for atmospheric ice particles*, *Appl. Opt.,* **35**, 4291-4296.

Macke, A, J Muller, and E Rasche. 1996: Single scattering properties of atmospheric crystals. *J. Atmos. Sci.,* **53**, 2813-2825.

Minnis, P., U. Schumann, D. R. Doelling, K. M. Gierens, and D. W. Fahey,1999: Global distribution of contrail radiative forcing, *Geophys. Res. Lett.*, **26**(13), 1853–1856.

Mishchenko, M. I., and L. D. Travis, 1994: T-matrix computations of light scattering by large spheroidal particles, *Opt. Commun.,* **109**, 16-21.

Myhre, G., M. Kvalevag, G. Radel, J. Cook, K. P. Shine, H. Clark, F. Karcher, K. Markowicz, A. Kardas, P. Wolkenberg, Y. Balkanski, M. Ponater, P. Forster, A. Rap, R. R. de Leon, 2009: Intercomparison of radiative forcing calculations of stratospheric water vapour and contrails, *Meteorol. Z.* **18***,* 585-596.

Myhre, G. and F. Stordal, 2001: On the tradeoff of the solar and thermal infrared radiative impact of contrails, *Geophys. Res. Lett.*, **28**(16), 3119–3122.

Penner, J. E., D. H. Lister, D. J. Griggs, D. J. Dokken, and M. McFarland, Eds., 1999: Aviation and the Global Atmosphere. *Cambridge University Press*, 365 pp.

Ponater, M., S. Marquart, and R. Sausen, 2002: Contrails in a comprehensive global climate model: Parametrization and radiative forcing results. *J. Geophys. Res.*, **107**(D13), doi:10.1029/2001JD000429.

Rädel, G., and K. P. Shine, 2008: Radiative forcing by persistent contrails and its dependence on cruise altitudes, *J. Geophys. Res.*, **113**, D07105, doi:10.1029/2007JD009117.

Sausen, R., I. Isaksen, V. Grewe, D. Hauglustaine, D.S. Lee, G. Myhre, M.O. Köhler, G. Pitari, U. Schumann, F. Stordal and C. Zerefos, 2005: Aviation radiative forcing in 2000: An update on IPCC (1999). *Meteorol. Z.,* **14**, 555-561.

Strauss, B. , Meerkoetter, R. , Wissinger B. , Wendling P. ,Hess M., 1997: *On the regional climatic impact of contrails : microphysical and radiative properties of contrails and natural cirrus clouds*, *Ann. Geophys.*, **15**, 1457-1467.

Stephens, G. L. and P. J. Webster, 1981: Clouds and climate: sensitivity of simple systems. *J. Atmos. Sci.,* **38**, 235-245.

Sun, W., Q. Fu, and Z. Chen, 1999: Finite-Difference Time-Domain Solution of Light Scattering by Dielectric Particles with a Perfectly Matched Layer Absorbing Boundary Condition, *Appl. Opt.*, **38**, 3141-3151.

Yang, P., H. Wei, H.-L. Huang, B. A. Baum, Y. X. Hu, G. W. Kattawar, M. I. Mishchenko, and Q. Fu, 2005: Scattering and absorption property database for nonspherical ice particles in the

near- through far-infrared spectral region, *Appl. Opt.*, **44**, 5512-5523.

Yang, P., K. N. Liou, K. Wyser, and D. Mitchell, 2000: Parameterization of the scattering and absorption properties of individual ice crystals, *J. Geophys. Res.*, **105**(D4), 4699–4718.

Yang, P., and K. N. Liou, 1996: Finite-difference time domain method for light scattering by small ice crystals in three-dimensional space, *J. Opt. Soc. Am. A,* **13**, 2072-2085.